

The effect of structural distortions on the electronic structure of carbon nanotubes

Alain Rochefort^{a,1}, Dennis R. Salahub^{a,b,2}, Phaedon Avouris^{c,3}

^a Centre de Recherche en Calcul Appliqué (CERCA), 5160 Boul. Décarie, Bureau 400, Montréal, Québec H3X 2H9, Canada

^b Département de Chimie, Université de Montréal, C.P. 6128, Succ. Centre-Ville, Montréal, Québec H3C 3J7, Canada

^c IBM Research Division, T.J. Watson Research Center, P.O. Box 218, Yorktown Heights, NY 10598, USA

Received 19 June 1998; in final form 24 September 1998

Abstract

We calculated the effects of structural distortions on the electronic structure of carbon nanotubes. The main effect of nanotube bending is an increased mixing of σ and π states. This mixing leads to an enhanced density-of-states in the valence band near the Fermi energy. While in a straight tube the states accessible for electrical conduction are essentially pure $C(2p_\pi)$ states, they acquire significant $C(2sp_\sigma)$ character upon bending. Bending also leads to a charge polarization of the C–C bonds in the deformed region reminiscent of interface dipole formation. Scattering of conduction electrons at the distorted regions may lead to electron localization. © 1998 Elsevier Science B.V. All rights reserved.

1. Introduction

Carbon nanotubes are an interesting class of nanostructures which can be thought of as arising from the folding of a graphene sheet. Depending on the width of the graphene sheet and the way it is folded, a variety of different nanotube structures are formed. The nanotubes are usually described using the chiral vector: $C_h = n\vec{a}_1 + m\vec{a}_2$, where \vec{a}_1 and \vec{a}_2 are unit vectors of the hexagonal honeycomb lattice and n, m are integers, and a chiral angle θ which is the angle of the chiral vector with respect to the zigzag direction of the graphene sheet [1,2]. The one-dimensional electronic structure of a nanotube with indices (n, m) can be predicted on the basis of

the two-dimensional electronic structure of graphite. Armchair (n, n) nanotubes have a band degeneracy between the highest π valence band and the lowest π^* conduction band at $k = \pm(2/3)(\pi/a_0)$, where these bands meet the Fermi level, and should show metallic behavior. Among the other (n, m) nanotubes, the ones with $n - m = 3i$ (where i is an integer) should also be metallic, while the rest should have a band-gap and, therefore, be semiconductors [1,2]. Recent STM spectroscopy experiments verified these predictions [3,4]. Their electrical properties coupled with the superb mechanical strength of the nanotubes [5,6] makes these materials promising candidates for use as ideal one-dimensional conductors, if ballistic transport can be achieved or, in the case of semiconducting tubes, as key building elements of novel nanoelectronic devices [7,8].

The above discussion of the properties of carbon nanotubes is based on the assumption that they have

¹ E-mail: rochefor@cerca.umontreal.ca

² E-mail: dennis.salahub@umontreal.ca

³ Corresponding author. E-mail: avouris@us.ibm.com

the perfect symmetry expected for a free nanotube. Nanotubes, however, are usually studied and utilized while being supported on a solid substrate. Studies of supported nanotubes using atomic force microscopy [9] and molecular mechanics calculations [10] show that supported nanotubes can undergo significant axial and radial distortions. The nanotubes tend to bend so as to conform to the morphology of the substrate and thus optimize the Van der Waals adhesion forces. Similarly, the side of the nanotube in contact with the surface may flatten so as to optimize the contact area. The extent of the above distortions depends on the balance between the increased adhesion and the rise in strain energy produced by the distortions. These structural distortions can, in turn, modify the nanotube's electronic structure and electrical transport properties. For example, a reduction in symmetry may result in the lifting of degeneracies. An increased curvature can enhance σ - π mixing and rehybridization, while bond strain can modify the band-gap of semiconducting tubes. These effects may produce local barriers at the distortion regions and affect electrical transport. Previous theoretical work on this problem [11] focused only on the π electrons, ignoring the σ electrons and the possibility of π - σ mixing, and concluded that the effects of bending distortions on electronic structure are insignificant. Experimentally, bends in quantum wires produced by patterning of two-dimensional electron-gas systems have been shown to affect transport and lead to interesting interference phenomena [12,13]. It is thus likely that similar effects may be induced by bends in nanotubes and be observable in low temperature transport experiments.

Here we explore the effects of structural distortions on the electronic structure of nanotubes by performing Extended Hückel calculations on straight and bent armchair (6,6) single-wall nanotubes. Important changes in the local density of states (LDOS) of σ and π electrons and increased π - σ mixing are observed to develop as the nanotube is distorted. These changes become stronger with increasing bending angle. In addition, a charge polarization of the C-C bonds in the distorted regions is observed. The electronic structure changes are expected to have important implications for the low temperature electrical transport properties of the nanotubes, and should also affect locally their chemical reactivity.

2. Computational details

Electronic structure calculations were performed on a 972 atom cluster model (948 C and 24 H that saturate the dangling bonds at the ends) of a (6,6) nanotube using the extended Hückel method [14]. The parameters used for carbon and hydrogen were: C_{2s} ($H_{ii} = -21.4$ eV, $\zeta = 1.625$), C_{2p} ($H_{ii} = -11.4$ eV, $\zeta = 1.625$), and H_{1s} ($H_{ii} = -13.6$ eV, $\zeta = 1.3$), where H_{ii} and ζ are the orbital energy and Slater exponents, respectively.

In the undistorted nanotube, the C-C and C-H bond lengths were fixed at the values obtained for bulk graphite [15] that are 1.42 and 1.09 Å, respectively. We have built models with bending angles of 30, 45 and 60° using a constant length segment in the middle of the tube to introduce the distortion. Prior to the electronic structure calculations, the geometry of the bent nanotubes was optimized with the molecular mechanics program TINKER [16] employing the MM3 force field [17]. In the structural relaxation and optimization process, the first five sections (a section is defined as a single circular plane of carbon atoms that are packed along the length of the nanotube) at the two ends of the nanotube were kept fixed in order to maintain the bending angle. In the molecular mechanics calculations, we used the MM3 alkene parameters except for the bond length parameter which we modified from that of an alkene (1.33 Å) to that of bulk graphite (1.42 Å). Density of states (DOS) plots were generated by convoluting the computed electronic structure with a 50:50 combination of Gaussian and Lorentzian functions. In order to analyze the origin of the band states, we performed a series of projections of the DOS where each molecular orbital was weighted by the contribution obtained from a Mulliken analysis of specific carbon atoms.

3. Results and discussion

Fig. 1 shows the computed electronic structure of a perfect (6,6) armchair nanotube model. This model contains 948 carbon atoms distributed in 79 circular sections. The overall DOS spectrum shows high binding energy (BE) states extending from -22 to -12 eV that are mainly σ -bond states involving C(2s) orbitals. The σ -bond states associated with

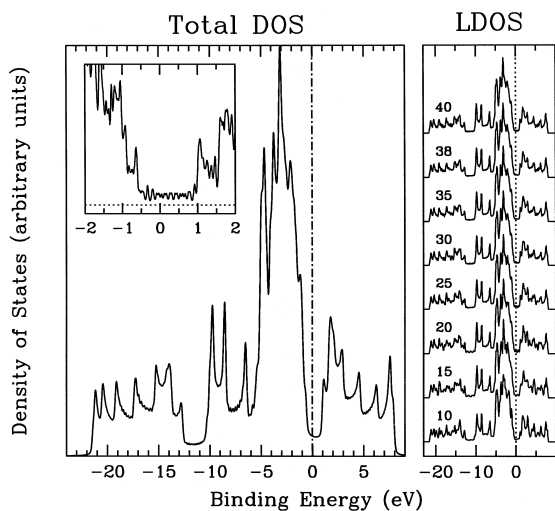


Fig. 1. Total (DOS) and local density of states (LDOS) diagrams of a straight armchair (6,6) nanotube (resolution = 0.2 eV). The indices in the LDOS diagram give the relative position of the carbon atoms in the nanotube structure (1: boundary; 40: middle of the nanotube). The inset gives an expanded view of the DOS near the Fermi level ($E = 0$ eV). The zero of the DOS scale is indicated by the horizontal line, and the energy resolution is 0.05 eV.

C(2p) orbitals lie at lower BE between -12 and 0 eV with respect to the Fermi energy (E_F). The fine structure visible in the high BE region involves van Hove singularities characteristic of one-dimensional systems [18]. Each of these peaks is characterized by a specific number of nodes in the wavefunction along the circumference of a single nanotube section, while the $1/\sqrt{E}$ tail reflects the free electron character along the tube axis. The more intense DOS bands between -6 and 0 eV are due to overlapping π - and σ -bond states, with the π states centered at a slightly lower binding energy. The set of DOS bands between 0 and 8 eV are essentially π^* states. The σ^* states (not shown) extend above 10 eV. The valence and conduction band states near the 'gap' edges have π character; electric transport involves π electrons. A more detailed view of the DOS in the region around the Fermi level is shown in the inset of Fig. 1.

The local density of states (LDOS) profiles presented in Fig. 1 where the projection is summed over the contribution of the 12 carbon atoms contained in a particular section of the tube shows that the elec-

tronic structure along the tube is quite uniform. The similarity of the LDOS profiles indicates that the wavefunction of this finite size tube is delocalized over its entire length.

Fig. 2 shows the model structures used to evaluate the effects of bending on the electronic properties of carbon nanotubes. The following approach is used to generate the 30° , 45° and 60° bend models: a section of constant length in the middle of the tube is bent and the atomic structure of the nanotube is then optimized with molecular mechanics. As the bending angle increases, the deformation of the atomic structure of the tube increases, particularly in the central region of the tube. The 30° bend induces a compression of the C–C bonds in the inner side of the tube while the bonds on the outer side are stretched. The general tubular shape, however, remains essentially intact in both straight and bent regions. After a 45° bend, the increased compression of C–C bonds in the center of the nanotube leads to a flattening of its cross-section. Further bending increases this flattening to the point where the force between opposite nanotube walls becomes high enough to induce the formation of a kink as in the 60° model of Fig. 2. The front views of the central sections of the bent tube models clearly show the drastic structural deformations that occur as the bending angle is increased from 45° to 60° .

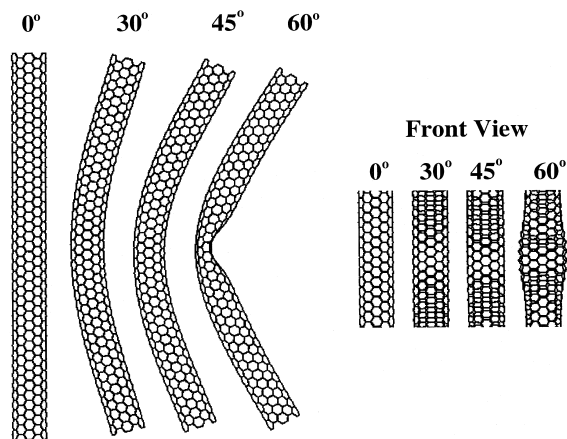


Fig. 2. Structures of bent (6,6) nanotubes optimized using molecular mechanics. The bending angles are (from left) 0° , 30° , 45° and 60° . A front view of the most central sections of bent models is also shown.

The changes in the electronic structure (from -25 to 10 eV) induced by the bending of the armchair (6,6) nanotube appear weakly in the total density of states spectrum. This is because the deformed region is relatively small compared to the total length of the nanotube. On the other hand, the LDOS along the nanotube length, i.e. the LDOS generated by adding the contributions of the 12 carbon atoms contained in a particular section of the nanotube, provides a much clearer view of the changes brought about by bending. As already discussed, in a straight (0°) nanotube there is no obvious variation of the LDOS along its length (Fig. 1). Upon bending, the most obvious change is a broadening of the fine structure of the overlapping σ - π states near E_F , which becomes particularly large in the 60° bent example. Far from the distorted region, the LDOS profiles are very similar (in terms of band position and structure) in all bent nanotube models. In the distorted segment of the tube (i.e. near the central section), the fine structure of the σ - π band disappears. The σ -bond states at higher binding energy arising from a combination of C(2s) orbitals are similarly altered. In general, σ bonds in the bent region appear to be the most perturbed by the deformation, while π bonds are affected to a lesser extent.

Another interesting result of the deformation involves the distribution of net charge along the length of the nanotube shown in Fig. 3. Upon increasing the bending angle from 0° to 60° , the net charge fluctuation rises. Furthermore, the position in the bent region where the largest fluctuations are observed changes with bending angle. A smooth 30° bending leads to a broad distribution of small charges among all carbon atoms in the bent region. A bending of 45° gives a larger charge fluctuation in the innermost deformed region. Finally, the kink in the 60° bent nanotube has a particularly dramatic effect on both the magnitude and the spatial extent of the net charge distribution leading to large charge fluctuations displaced toward the central edges of the kinked region. In general, the largest fluctuations are found where the changes in the nanotube geometry (R_{C-C}) are most pronounced. This localization of charge fluctuations is directly related to the changes observed in the σ wavefunction discussed above; the larger fluctuations arise from an enhanced σ orbital

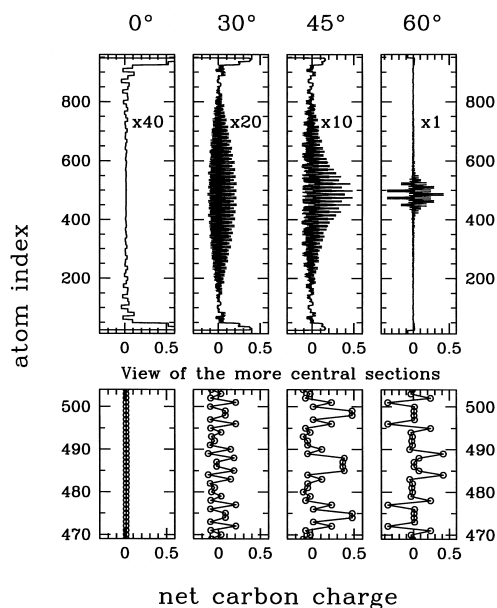


Fig. 3. Variation of the net charge distribution along the length of bent nanotubes. Atom indices give the relative position of the carbon atoms in the nanotube structure (a total of 948 carbon atoms distributed in 79 sections of 12 carbon atoms each were used).

contribution or, in other words, from an increased sp^2 - sp^3 rehybridization.

To investigate how the electrical transport properties of the nanotube may be affected by bending, we focus on the π states near E_F . The upper part of Fig. 4 shows an expanded view of the DOS in this energy range. Bending is found to induce an increased DOS near E_F (at about -1 eV BE). Furthermore, the DOS at E_F remains finite in all bent nanotubes studied. More informative are LDOS curves along the nanotube length. In the case of a straight tube, the lack of change in LDOS along the tube indicates that π and π^* states near E_F are not confined in a specific area but are delocalized along its length. Upon bending, small changes in the electronic structure are observed at the tube boundaries. These changes result from the relaxation of the atomic structure of the entire nanotube upon bending. The largest changes are found, however, at the centers of the nanotubes (Section 40), in particular in the kinked tube (60° angle). Fig. 4 shows an overall increase in the LDOS near E_F in the distorted regions of the nanotubes. Analysis of the wavefunction indicates

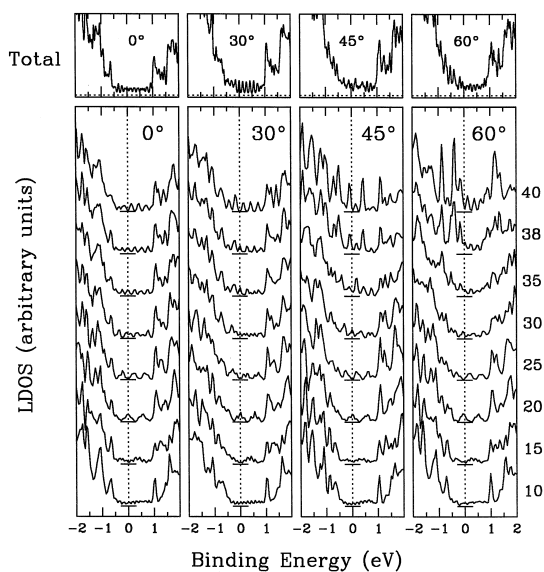


Fig. 4. Variation of DOS and LDOS near the Fermi level for several bent (6,6) armchair nanotubes (resolution = 0.05 eV). Indices give the relative position of the section in the nanotube structure (1: boundary; 40: middle of the nanotube).

that the induced density contains an increased contribution of $C(2sp_{\sigma})$ states. The shift of the valence band edge to higher energy and the increased $C(2sp_{\sigma})$ contribution can both be explained by a bending-induced π - σ hybridization. Such a rehybridization already exists to some extent in the straight tube due to its curvature [19] but becomes enhanced by further bending.

In conclusion, we have shown that the local electronic structure of carbon nanotubes is modified as a result of structural distortions. Such distortions can be the result of the interaction of the nanotubes with the topography of the substrate they are placed on [10], with the metal electrodes used to monitor their electrical properties [20], or as a result of controlled manipulation [9]. Two types of perturbations of the electronic structure as a result of bending are predicted by our calculations. First, a modification of the LDOS in the deformed region of the nanotube leading to an increased DOS near E_F and a shift of the valence band edge to a lower binding energy. These effects are due to increased π - σ hybridization. Discussion of electrical transport in distorted tubes must take into account this hybridization. Secondly, we observe a charge polarization of the C-C

bonds in the deformed region. The magnitude of this polarization increases with the bending angle and is particularly severe upon kink formation. The above changes in the local electronic structure are expected to scatter the conduction electrons at the deformed regions leading to carrier localization, especially at low temperatures. Truly ballistic transport in nanotubes may require perfectly straight tubes [21]. This conclusion is supported by recent experiments by Bezryadin et al. [20] who examined the electrical behavior of a chiral single-wall nanotube draped over a set of several Pt electrodes. Their studies indicated that electrically the nanotube was broken into a series of isolated islands as a result of barriers generated by the bending of the tube over the raised electrodes, as suggested in Ref. [9].

Acknowledgements

We would like to thank T. Hertel for many helpful discussions.

References

- [1] R. Saito, M. Fujita, G. Dresselhaus, M.S. Dresselhaus, *Appl. Phys. Lett.* 60 (1992) 2204.
- [2] M.S. Dresselhaus, G. Dresselhaus, P.C. Eklund, *Science of Fullerenes and Carbon Nanotubes*, Academic Press, San Diego, CA, 1996.
- [3] J.W.G. Wildöer, L.C. Venema, A.G. Rinzier, R.E. Smalley, C. Dekker, *Nature* 391 (1998) 59.
- [4] T.W. Odom, J.-L. Huang, P. Kim, C.M. Lieber, *Nature* 391 (1998) 62.
- [5] M.M. Treacy, T.W. Ebbesen, J.M. Gibson, *Nature* 381 (1996) 678.
- [6] E.W. Wong, P.E. Sheehan, C.M. Lieber, *Science* 277 (1997) 1971.
- [7] S.J. Tans, R.M. Verschueren, C. Dekker, *Nature* 393 (1998) 49.
- [8] R. Martel, T. Schmidt, H.R. Shea, Ph. Avouris, *Appl. Phys. Lett.* 73 (1998) 2447.
- [9] T. Hertel, R. Martel, Ph. Avouris, *J. Phys. Chem. B* 102 (1998) 910.
- [10] T. Hertel, R. Walkup, Ph. Avouris, *Phys. Rev. B* 58 (15 Nov. 1998).
- [11] C.L. Kane, E.J. Mele, *Phys. Rev. Lett.* 78 (1997) 1932.
- [12] J.C. Wu, M.N. Wybourne, *Appl. Phys. Lett.* 59 (1991) 102.
- [13] A. Weisshaar, J. Lary, S.M. Goodnick, *Appl. Phys. Lett.* 55 (1989) 2114.

- [14] G. Landrum, YAeHMOP Yet Another Extended Hückel Molecular Orbital Package, Cornell University, Ithaca, NY, 1995.
- [15] Gmelin Handbuch der Anorganischen Chemie, vol. 14B/2, 8th edition, Verlag Chemie, Weinheim, 1968, p. 413.
- [16] Y. Kong, J.W. Ponder, *J. Chem. Phys.* 107 (1997) 481.
- [17] N.L. Allinger, Y.H. Yuh, J.-H. Lii, *J. Am. Chem. Soc.* 111 (1989) 8551.
- [18] N.W. Ashcroft, N.D. Mermin, *Solid States Physics*, Saunders College Publ., Philadelphia, PA, 1976.
- [19] X. Blase, L.X. Benedict, E.L. Shirley, S.G. Louie, *Phys. Rev. Lett.* 72 (1994) 1878.
- [20] A. Bezryadin, A.R.M. Verschueren, S.J. Tans, C. Dekker, *Phys. Rev. Lett.* 80 (1998) 4036.
- [21] S. Frank, P. Poncharal, Z.L. Wang, W.A. de Heer, *Science* 280 (1998) 1744.